http://dx.doi.org/10.5935/0103-5053.20140118

J. Braz. Chem. Soc., Vol. 25, No. 8, 1365-1371, 2014.
Printed in Brazil - ©2014 Sociedade Brasileira de Química
0103 - 5053 $6.00+0.00

Article

Catalytic Dehydration of Ethanol to Ethylene over Alkali-Treated HZSM-5 Zeolites

Qingtao Sheng,[a] Shaoqing Guo,[,b] Kaicheng Ling[a] and Liangfu Zhao*[,c]*

[a]*College of Chemistry and Chemical Engineering, Taiyuan University of Technology, 030024 Taiyuan, Shanxi, P. R. China*

[b]*School of Environment and Safety, Taiyuan University of Science and Technology, 030024 Taiyuan, Shanxi, P. R. China*

[c]*Institute of Coal Chemistry, Chinese Academy of Sciences, 030001 Taiyuan-Shanxi, P. R. China*

A performance catalítica de catalisadores HZSM-5 com tratamento alcalino foi investigada em um microrreator contínuo de leito fixo. As propriedades dos catalisadores HZSM-5 de origem e modificados foram caracterizadas por difração de raio X (XRD), espectroscopia de emissão atômica com plasma indutivamente acoplado (ICP-AES), adsorção de N_2 e dessorção programada por temperatura de NH_3 (NH_3-TPD). Os resultados mostraram que o tratamento alcalino é um método adequado para modificar o catalisador HZSM-5 para a desidratação do etanol a etileno. O catalisador HZSM-5 tratado com 0.4 mol L^{-1} NaOH apresentou alta atividade e boa estabilidade. As performances catalíticas melhoradas dos catalisadores com tratamento alcalino são atribuídas, principalmente, aos mesoporos criados e à diminuição de sítios ácidos fortes durante o tratamento alcalino.

The catalytic performance of alkali-treated HZSM-5 catalysts was investigated in a continuous fixed-bed microreactor. The properties of the parent and modified HZSM-5 catalysts were characterized by X-ray diffraction (XRD), inductively coupled plasma atomic emission spectroscopy (ICP-AES), N_2 adsorption and temperature programmed desorption of NH_3 (NH_3-TPD). The results show that the alkali treatment is a suitable method to modify the HZSM-5 catalyst for ethanol dehydration to ethylene. The HZSM-5 catalyst with 0.4 mol L^{-1} NaOH shows high activity and good stability. The improved catalytic performances of alkali-treated catalysts are mainly attributed to the created mesopores and the decreased number of strong acid sites during the alkali treatment.

Keywords: HZSM-5, alkali treatment, ethanol dehydration, desilication

Introduction

Ethylene, which is conventionally produced by thermal cracking of petroleum, is a key intermediate used in the production of ethylene oxides, polyethylene, vinyl chloride, and styrene. In recent years, it has been necessary to look for some new sustainable ways to produce ethylene because of the global energy crisis combined with environmental problems. Therefore, the catalytic dehydration of ethanol to ethylene has attracted more and more attention due to its lower temperature process and the raw material of ethanol that can be obtained easily from renewable agricultural resource by fermentation. It is crucial to find an effective catalyst and some catalysts have been tested in the literature for dehydration of ethanol to ethylene, such as γ-alumina,[1] heteropolyacid catalysts[2] and zeolites.[3-5] Among them, HZSM-5 zeolite is interesting because of the lower temperature and higher ethylene yield.[6-8] However, the deactivation of the catalyst caused by the strong acidity and the intracrystalline diffusion limitation in HZSM-5 zeolite micropores leads to the unfeasible process for industrial applications.[9]

HZSM-5 zeolite has been treated with steaming, acid-leaching and modified by doping with metals, resulting in modified acidic properties, formation of mesopores and lower deactivation of the catalyst.[10-12] However, a rather limited mesoporosity development can be obtained by these methods.[13-16] Meanwhile, a higher reaction temperature is needed for these methods.[13-16] Recently, alkali-treated zeolites with NaOH have been studied widely as a relatively new strategy for creating mesopores without destroying the micropores.[17-20] The formed mesopores in alkali-treated HZSM-5 are more beneficial to the diffusion of reactants or products during the reaction and the modified HZSM-5 catalysts present higher catalytic activities in some reactions.[21-24] This has been proved in the literature; for

*e-mail: guosq@sxicc.ac.cn; lfzhao@sxicc.ac.cn

example, Jin *et al.*[22] observed that mesopores in alkali-treated HZSM-5 resulted in higher catalytic activities and longer lifetime for selectivity synthesis of 2,6-dimethylnaphthalene. Bjørgen *et al.*[24] found that the formation of mesopores and modification of acidic properties enhanced catalytic performance in the conversion of methanol to gasoline. Gayubo *et al.*[25] reported that the transformation of bioethanol into hydrocarbons (in particular C_3-C_4 olefins and BTXE) achieved a high selectivity of propene and butanes. However, little work has been carried out to investigate the catalytic performance of alkali-treated HZSM-5 zeolites on ethanol dehydration to ethylene.

In this paper, the acidity and pore structure of alkali-treated HZSM-5 were investigated. The catalytic performances of modified HZSM-5 catalysts for ethanol dehydration to ethylene were examined with emphasis on the activity, stability and regenerability of the catalysts.

Experimental

Catalysts preparation

HZSM-5 zeolite with SiO_2/Al_2O_3 molar ratio of 39.4 was supplied by the Catalyst Plant of Nankai. The samples were treated with solutions of 0.2, 0.4, 0.8 and 1.0 mol L^{-1} NaOH for 2 h at 75 °C, respectively. After filtration, washing and drying, the alkali-treated samples were ion-exchanged into the H-form by three consecutive exchanges in 0.1 mol L^{-1} NH_4NO_3 solution, and calcined at 550 °C for 5 h. The alkali-treated HZSM-5 samples were marked as ATx (where x denotes the NaOH concentration).

Catalysts characterization

X-ray diffraction (XRD) patterns were recorded on a D/max-2500 X-ray diffractometer with Cu-K_α radiation at room temperature and instrumental settings of 40 kV and 40 mA. The scanning range was from 5° to 50°. The relative crystallinity was calculated according to the intensities of three peaks at 2θ values of 23.07°, 23.28° and 23.90°. The three peak intensities of the parent HZSM-5 zeolite were considered to be 100% crystallinity.

Inductively coupled plasma optical emission spectrometry (ICP-AES)(JA1100 inductively coupled plasma quantometer) was used for the determination of the Si and Al contents in each sample.

N_2 adsorption-desorption isotherms were recorded on a Micromeritics Tristar-3000 instrument at liquid nitrogen temperature of −196 °C. Before the analysis, each sample was evacuated at 300 °C for 8 h. The total surface area was calculated according to the BET isothermal equation, and the micropore volume and external surface area were evaluated by the t-plot method.

The acid properties were examined by temperature programmed desorption of NH_3 (NH_3-TPD) with a thermal conductivity detector (TCD). About 100 mg of samples was pretreated at 500 °C in Ar flow (40 mL min^{-1}) for 1 h, and then cooled to 40 °C. The adsorption of pure NH_3 was performed at this temperature. When saturated adsorption is achieved, the system is swept by Ar (40 mL min^{-1}) for 1 h. The NH_3-TPD curves of the samples were recorded under Ar flow by heating from 40 °C to 600 °C at the rate of 5 °C min^{-1}.

The thermogravimetric studies of the catalysts after reaction were carried out using a NETZSCHSTA 409 PC thermoanalyzer with the temperature rise from room temperature to 800 °C at a heating rate of 10 °C min^{-1} in air flow.

Catalytic testing

Dehydration of ethanol was tested in a fixed bed reactor with an inner diameter of 6 mm under atmospheric pressure. A stainless steel tubular reactor was placed into a temperature programmed tubular furnace. After alkali treatment, 1.0 g catalyst was placed into the middle of the reactor. The reactant mixture of ethanol and water [the ethanol concentration is 20(v)% to simulate bioethanol] was injected into the reactor with nitrogen flow (40 mL min^{-1}). The weight hourly space velocity (WHSV) of ethanol was 2.37 h^{-1}. The reaction products were analyzed using a gas chromatograph (GC-9560, Shanghai Haixin GC) using a GDX-103 packed column, N_2 as carrier gas and flame ionization detector (FID) detector at oven temperature of 120 °C. The ethylene selectivity (S_E) and the conversion of ethanol (X_{EtOH}) were adopted to estimate the catalytic performance. S_E is defined as the molar ratio of ethylene to the total converted ethanol; X_{EtOH} is defined as the molar ratio of converted ethanol to the total injected ethanol. The reproducibility of the experiments was tested at the same experimental conditions for two or three times. No significant difference on the results was observed and the results are reproducible with a high accuracy.

Results and Discussion

Catalysts characterization

The XRD patterns of the parent and the treated HZSM-5 with different NaOH concentrations are shown in Figure 1. From Figure 1, it can be seen that all samples exhibit typical MFI structure and no additional phase appears. However,

the peak intensity decreases with the increase of NaOH concentration, which suggests that the concentration of alkali influences significantly the relative crystallinity of HZSM-5. At 1.0 mol L^{-1} of NaOH, the characteristic diffraction peaks attributed to HZSM-5 still remain, but the relative crystallinity decreases rapidly to 46.1% (see Table 1). This is mainly attributed to the removal of silicon species from the framework during the alkali treatment process, which may destroy the lattice structure and decrease the relative crystallinity.

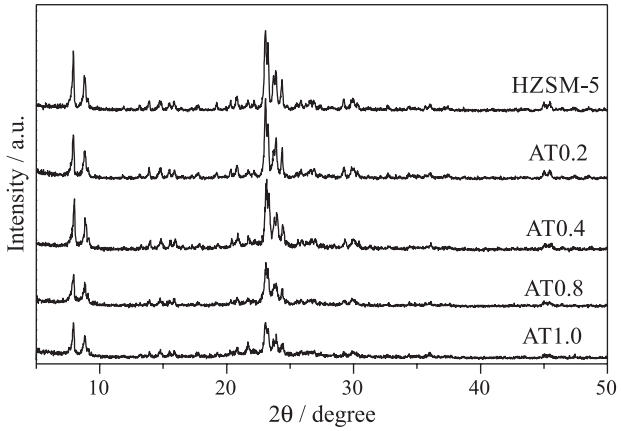

Figure 1. XRD patterns of the parent and alkali-treated HZSM-5.

It can be seen from Table 1 that the molar ratio of SiO_2/Al_2O_3 dramatically decreases from 39.4 to 30.5 with the NaOH concentration increasing from 0 to 0.4 mol L^{-1}, indicating a preferential removal of Si species during the alkali-treatment. It is in agreement with a previous report.[26] The preferential removal of Si results in the lower molar ratio of SiO_2/Al_2O_3 in the zeolites. However, the ratio of SiO_2/Al_2O_3 bounces to 32.0 at 0.8 mol L^{-1} of NaOH. This may result from the occurrence of dealumination during the desilication of zeolite.[27] Additionally, according to the report of Li,[28] the dissolved Si in NaOH solution may deposit on the surface of HZSM-5 as amorphous Si species (backward reaction). Both the dealumination and the deposit of Si species from the solution may be the main factors leading to the increase in the molar ratio of SiO_2/Al_2O_3.[29] With increasing alkali concentration to 1.0 mol L^{-1}, more framework Al attached to the framework Si become instable and easy to remove after the alkali treatment. This leads to the decrease of the SiO_2/Al_2O_3 molar ratio of AT1.0.[30]

The N_2 adsorption-desorption isotherms of all samples are shown in Figure 2. The isotherm of the parent HZSM-5 represents its microporous nature with a plateau at high relative pressure. The samples treated with NaOH solution in the concentrations of 0.2 mol L^{-1}, 0.8 mol L^{-1} and 1.0 mol L^{-1} have a slightly increase in nitrogen uptake within the relative pressure range between 0.4-1.0, indicating the formation of new mesopores. Surprisingly, there is a sharp increase of nitrogen uptake for the sample treated by 0.4 mol L^{-1} NaOH within the same pressures range, indicating the most abundant mesopores for the AT0.4 sample.

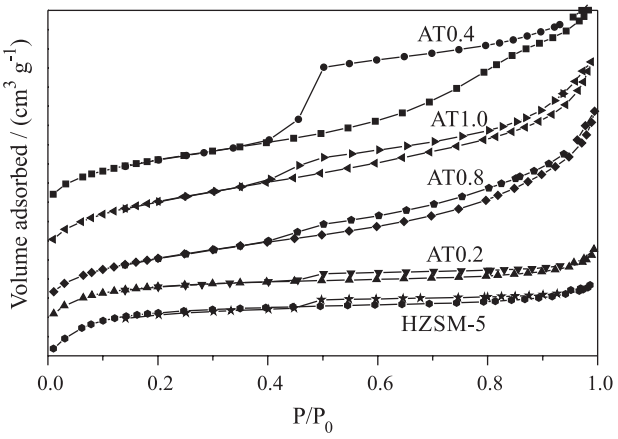

Figure 2. N_2 adsorption/desorption isotherms of the parent HZSM-5 and alkali-treated HZSM-5.

Table 1 shows that the surface area (S_{BET}) and the micropore volume (V_{micro}) decrease with increasing NaOH concentration. The external surface area (S_{ext}) increases markedly from 81 $m^2 g^{-1}$ of the parent HZSM-5 to 125 $m^2 g^{-1}$ of the AT0.4. The mesopore volume (V_{meso}) increases from 0.06 $cm^3 g^{-1}$ for the parent HZSM-5 to 0.18 $cm^3 g^{-1}$ for

Table 1. Properties of the parent and alkali-treated samples

Sample	S_{BET}[a] / ($m^2 g^{-1}$)	S_{ext} / ($m^2 g^{-1}$)	S_{mic} / ($m^2 g^{-1}$)	V_{micro}[b] / ($cm^3 g^{-1}$)	V_{meso}[c] / ($cm^3 g^{-1}$)	SiO_2/Al_2O_3	Cristallinity
HZSM-5	355	81	274	0.13	0.06	39.4	100
AT0.2	341	92	249	0.11	0.08	38.2	92.2
AT0.4	330	125	205	0.09	0.18	30.5	83.2
AT0.8	326	107	219	0.07	0.17	32.0	58.5
AT1.0	272	122	150	0.06	0.17	25.6	46.1

[a]BET method; [b]volume adsorbed at $P/P_0 = 0.99$; [c]t-plot method.

AT0.4, indicating the formation of mesopores after alkali treatment. Both the S_{ext} and the V_{meso} reach their maximum for the AT0.4. The V_{meso} decreases slightly from 0.18 $cm^3\ g^{-1}$ for the AT0.4 to 0.17 $cm^3\ g^{-1}$ for AT0.8 or AT1.0, which is due to the backward deposition of amorphous Si on some mesopores or the collapse of zeolite framework.[28] In a word, AT0.8 sample has a mesopore volume very close to that of AT0.4, while its external surface is just slightly lower. The external surface area and mesopore volume of HZSM-5 is developed at 0.8 mol L^{-1} of NaOH, while AT0.4 with a largely developed mesopore is obtained at the suitable condition of alkali treatment.

Figure 3 shows the NH_3-TPD profiles of all samples. The similar curves for the parent HZSM-5 and AT0.2 in Figure 3 indicate that the acid sites are completely preserved after alkali treatment. However, the total acid sites of samples decrease significantly with increasing NaOH concentration, especially for the strong acid sites. Compared with the parent HZSM-5, the alkali-treated samples exhibit lower desorption temperature of strong acid sites, indicating the weakened strengths of acid sites. The relative acid densities are calculated according to the areas of the NH_3-TPD profiles, and the total acid densities for the samples is in the order of HZSM-5 ca. AT0.2 > AT0.4 > AT0.8 > AT1.0, indicating that the acid density of the samples decreases with increasing NaOH concentration. The decrease in acid density of the samples is mainly ascribed to the decrease of the strong acid sites presented at 300-500 °C in Figure 3. The decrease of the strong acid sites may be related to the removal of extra-framework Al during the alkali treatment.[30] In addition, the desilication might lead to the destabilization of micropore structure, even the collapse of zeolite framework, resulting in the decrease of the strong acid sites for the catalysts.[28] So, it can be concluded that the acidic properties of HZSM-5 were modified by the alkali treatment.

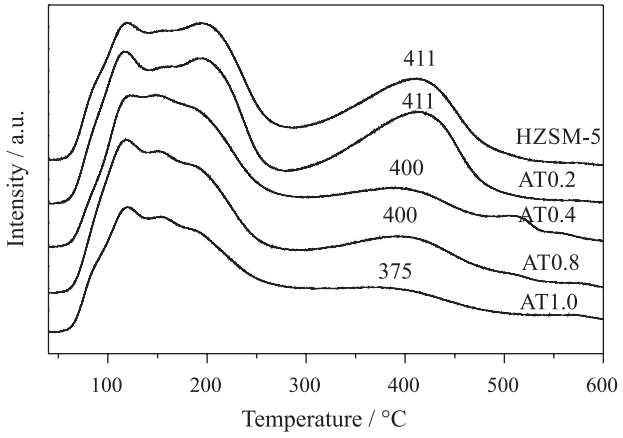

Figure 3. NH_3-TPD profiles of the parent and alkali-treated HZSM-5.

Effect of alkali treatment on catalytic dehydration of ethanol to ethylene

X_{EtOH} and S_E of the catalysts at different temperature are listed in Table 2. Table 2 shows that X_{EtOH} and S_E were lower at lower temperatures, which indicates that the dehydration of ethanol was incomplete at reaction temperatures < 265 °C. Generally, the ethanol dehydration into ethylene is an endothermic reaction and its main side reaction of ethanol dehydration into diethyl ether is a slightly exothermic reaction (the reaction equations are listed below).

$$C_2H_5OH \rightarrow C_2H_4 + H_2O \qquad +44.9\ kJ\ mol^{-1}$$
$$C_2H_5OH \rightarrow C_2H_5O\,C_2H_5 + H_2O \qquad -25.1\ kJ\ mol^{-1}$$

The increase of the reaction temperature favors the main reaction of the dehydration of ethanol to ethylene and improves the catalysts activity. The alkali-treated catalysts (except for AT1.0) show higher activity and selectivity to ethylene compared to the parent catalyst, which is mainly associated with the created mesopores and the moderate acidity. As stated previously, the mesopores volume and the external surface area (Table 1) for all treated samples increase. This leads to the increase of the adsorption sites located near the pore mouth on the external surface of zeolite and the promotion of the diffusion of reactant to the active sites.[17,31,32] Figure 3 shows that the total acid sites of alkali-treated samples decrease significantly. Meanwhile, the strength of acid sites is weakened compared to the parent HZSM-5, especially for the strong acid sites. The decrease in acidity of strong acid sites suppresses the side reactions to higher olefins, improving the selectivity to ethylene.

The selectivity to ethylene decreases with increasing NaOH concentration. This is attributed to the decrease of the acidity and the development of the mesopore, which leads to the higher production of diethyl ether. It should be noted that the SiO_2/Al_2O_3 ratio for all the modified HZSM-5 decreases compared to the parent catalyst. It may be indicated that the decreased SiO_2/Al_2O_3 ratio is beneficial for the ethanol dehydration. However, AT1.0 shows no significant improvement on the reaction. This might be caused by its lower relative crystallinity and surface area (see Figure 1 and Table 1).

The alkali-treated catalysts present higher activity and selectivity than those of the parent HZSM-5 when the reaction is carried out at lower temperatures (below 260 °C). In addition to their high external surface area and mesopore volume, their moderate acidity and lower SiO_2/Al_2O_3 ratio can promote the reaction. Among them, AT0.4 with higher mesopores volume and external surface

Table 2. The conversion and selectivity of alkali-treated HZSM-5 catalysts (%)

Temperature / °C	HZSM-5		AT0.2		AT0.4		AT0.8		AT1.0	
	X_{EtOH}	S_E	X_{EtOH}	S_E	X_{EtOH}	S_E	X_{EtOH}	S_E	X_{EtOH}	S_E
230	78.2	31.1	87.7	63.6	86.6	46.2	85.2	43.4	83.2	28.3
240	82.7	53.4	92.9	87.2	90.7	70.7	89.7	67.4	87.1	50.1
250	92.8	84.8	97.2	97.0	94.6	90.7	94.5	88.4	91.9	71.0
260	98.5	96.8	99.4	99.2	98.6	96.4	99.2	98.6	94.3	91.4
265	99.6	98.2	99.5	98.5	99.7	99.6	99.5	99.0	96.9	97.2

area exhibits the highest ethanol conversion and selectivity to ethylene at 265 °C.

The stability of alkali-treated catalysts on dehydration of ethanol

As mentioned previously, AT0.4 shows good catalytic performances. To study the catalytic stability of the AT0.4, the stability test of 170 h was carried out at 265 °C and the results are shown in Figure 4. For easy comparison, the stability test of the parent HZSM-5 at the same conditions was also carried out and the results are given in Figure 4.

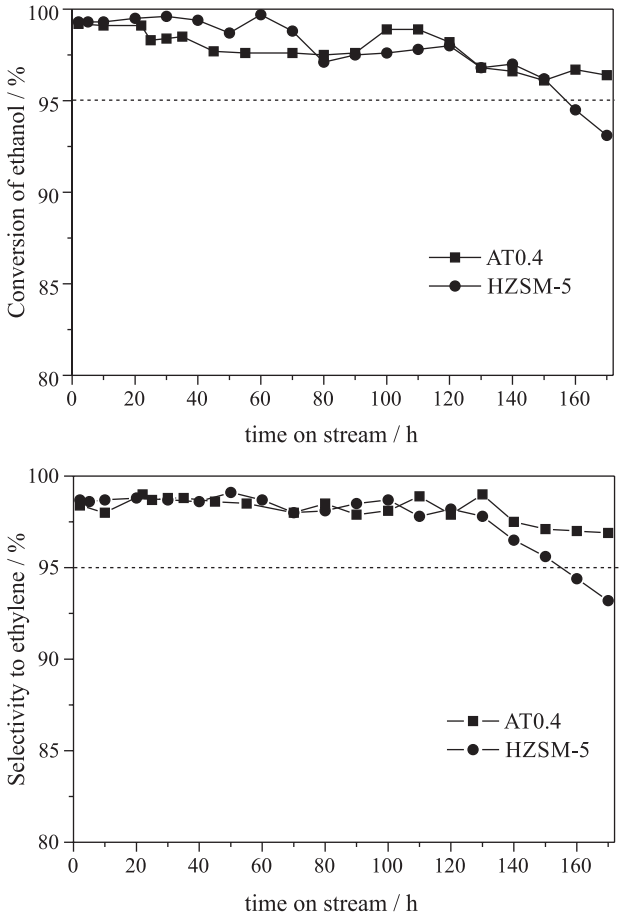

Figure 4. The lifetimes of the parent HZSM-5 and AT0.4 catalyst.

It is clear that both X_{EtOH} and S_E drop to 93% after reacting 170 h for the parent HZSM-5. In contrast, they are maintained at 97-98% for AT0.4. It means that AT0.4 shows more effective catalytic activity and much higher stability than the parent HZSM-5. To further study the stability of the AT0.4, the catalytic stability test of 350 h for AT0.4 was conducted. The results show that X_{EtOH} and S_E are still maintained at 95% after 350 h and no obvious deactivation is observed.

It is well known that the stability of zeolites in the reaction is associated with the catalyst deactivation. The zeolite with more strong acid sites is generally found to deactivate sharply due to the higher coke yields.[33,34] For the ethanol dehydration to ethylene, the strong acid sites are responsible for the polymerization of ethylene to form higher olefins and aromatics. Therefore, the deactivation of HZSM-5 zeolite is attributed to the coke formation, which covers the acid sites and blocks the micropores. For the parent HZSM-5, it has more strong acid sites than the AT0.4 does, which favors the polymerization of ethylene to form carbonaceous species that cover these sites and leads to the deactivation of the catalyst quickly. This is in agreement with the deactivation behavior of HZSM-5 reported in the literature.[9] For the AT0.4, the decrease in strong acid sites suppresses the coke formation and increases the lifetime of catalysts.[35] Therefore, the AT0.4 catalyst presents much stability and resistance to coke formation.

Actually, the coke in the parent HZSM-5 and AT0.4 is formed inevitably during the reaction. However, AT0.4 presents higher stability than the parent HZSM-5. The possible reason is that the newly created mesopores on AT0.4 favor the diffusion of reactants and products, thus decreasing the contact time of the reactants.[36] So, the light olefins produced during the reaction have to be quickly removed to avoid the further polymerization reaction. Meanwhile, the newly created mesopores may accommodate part of coke deposition, consequently suppressing the formation of the coke deposition in its inherent micropores to some extent. Therefore, as the coke deposition in the mesopores cannot hinder the feed and/or

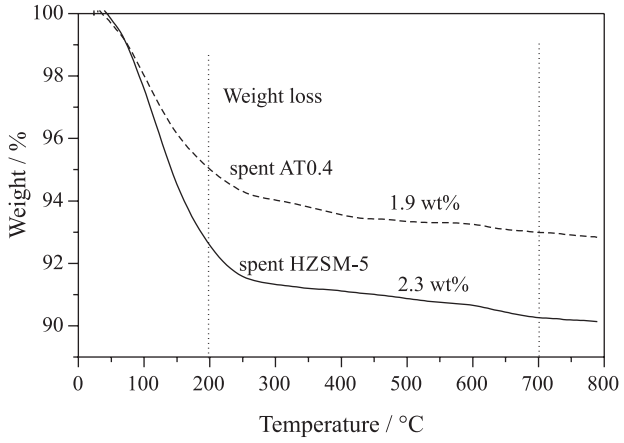

Figure 5. TG profiles of the spent HZSM-5 and the spent AT0.4 catalyst.

products diffusing from/to the active sites,[37] the AT 0.4 still shows higher activity at 350 h.

The TG analysis was performed on the spent HZSM-5 and the spent AT0.4 catalyst with reaction time of 170 h to investigate the coke deposition (see Figure 5). As seen in Figure 5, the two spent catalysts show the weight loss at the temperature range of 200-700 °C, which is ascribed to the burning of coke deposition. There is a difference in the amount of weight loss, 2.3 wt.% for the spent HZSM-5 and 1.9 wt.% for the AT0.4, indicating the coke deposition of the spent AT0.4 is lower than that of the spent HZSM-5. It indicates that the alkali treatment can inhibit the formation of the coke deposition, which can be responsible for the improvement of catalyst stability for AT0.4.

In brief, both the moderate number of strong acid sites and the newly created mesoropores of AT0.4 lead to the improvement of catalytic stability and coke-tolerance ability.

Catalytic performance of the regenerated catalyst

The regeneration of the spent catalyst of AT0.4 was conducted at temperature programming oven. The catalyst was put into the oven and heated to 400 °C for 2 h under air at the rate of 2.5 °C min^{-1}. After that, the temperature was raised to 500 °C and maintained for 4 h, and then cooled to room temperature. During the regeneration process, great part of the coke deposits were burnt and released out.

The stability of the regenerated catalyst was also tested at the same conditions as fresh catalyst. The results in Figure 6 show that X_{EtOH} and S_E for the regenerated catalyst are maintained around 98.7% and 98.6% at 170 h, respectively. To further study the stability of the regenerated AT0.4, the stability test of 350 h was also conducted and it still showed good catalytic performance. X_{EtOH} and S_E still keep 97% at 350 h. In comparison to the fresh catalyst, the regenerated catalyst exhibits a little lower X_{EtOH} and a higher S_E. At the same time, the regenerated catalyst exhibits better stability than the fresh catalyst.

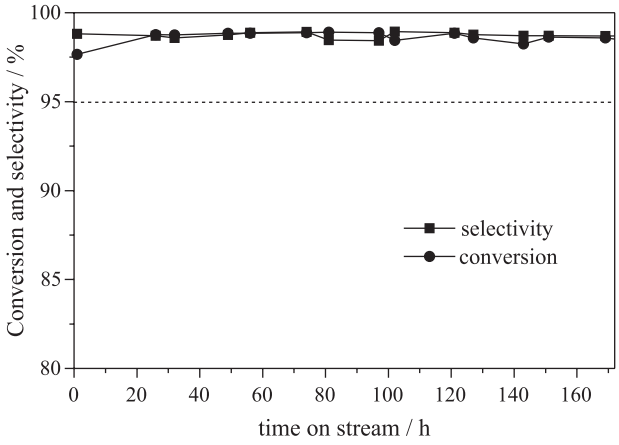

Figure 6. The lifetime of regenerated AT0.4 catalyst.

The decrease of the catalytic activity for AT0.4 is due to the coke deposition on the surface of the catalyst, which blocks the pore mouth of zeolite crystal. Generally, the coke deposition depletes strong acid sites preferentially.[38] During the process of regeneration, the coke deposition is burned to release out and the acid sites are recovered. However, the acid sites of the catalyst cannot be recovered completely after regeneration. Therefore, the acid sites of the regenerated catalyst decrease.[12] The decrease in acidity (especially strong acid sites) suppresses other side reactions and leads to the improvement of the selectivity to ethylene. At the same time, the decrease in acidity results in the decrease of coke formation and increases the lifetime of catalysts, which is in agreement with the discussion stated above. It is reported that some new mesopores are formed during the regeneration procedure.[39] The new mesopores formed can improve the diffusivity of the reactant and the product, leading to the increase of the selectivity to ethylene. In summary, the better S_E and stability of the regenerated AT0.4 is attributed to the decreased acidity and the increased number of mesopores after regeneration.

Conclusions

The alkali treatment is a suitable method to modify the HZSM-5 catalyst for ethanol dehydration to ethylene. The number of strong acid sites can be reduced and new mesopores can be created on the HZSM-5 catalyst during the alkali treatment process. The HZSM-5 catalyst with 0.4 mol L^{-1} NaOH exhibits high activity and good stability. The newly created mesopores favor the molecular diffusion and accommodate part of coke deposition, consequently

suppressing the formation of coke in the inherent micropores to some extent. The decrease in the number of strong acid sites after treatment suppresses the coke deposition. Meanwhile, the regenerated catalyst exhibits good catalytic performances.

Supplementary Information

Supplementary information is available free of charge at http://jbcs.sbq.org.br as PDF file.

Acknowledgments

This work was supported by the National High-tech R&D Program of China (863 Program) (2012AA051002).

References

1. Homer, A.; Perkins, P. P.; *J. Am. Chem. Soc.* **1925**, *47*,1163.
2. Varisli, D.; Dogu, T.; Dogu, G.; *Chem. Eng. Sci.* **2007**, *62*, 5349.
3. Jacobs, J. M.; Jacobs, P. A.; Uytterhoeven, J. B.; *US Patent 4670620* **1987**.
4. Talukdar, A. K.; Bhattacharyya, K. G.; Sivasanker, S.; *Appl. Catal., A* **1997**, *148,* 357.
5. Takahara, I.; Saito, M.; Matsuhashi, H.; Aritani, H.; Inaba, M.; Murata, K.; *J. Japan Petrol. Inst*. **2007**, *50*, 227.
6. Phillips, C. B.; Datta, R.; *Ind. Eng. Chem. Res.* **1997**, *36*, 4466.
7. Takahara, I.; Saito, M.; Inaba, M.; Murata, K.; *Catal. Lett.* **2005**, *105*, 249.
8. Takahara, I.; Saito, M.; Matsuhashi, H.; Inaba, M.; Murata, K.; *Catal. Lett.* **2007**, *113*, 82.
9. Schulz, J.; Bandermann, F.; *Chem. Eng. Technol.* **1994**, *17*, 179.
10. Fan, Y.; Bao, X. J.; Lin, X. Y.; *J. Phys. Chem. B* **2006**, *110,* 5411.
11. Mao, D. S.; Guo, Q. S.; Meng, T.; *Acta Phys. Chim. Sin.* **2010**, *26*, 338.
12. Jia, O. Y.; Kong, F. X.; Su, G. D.; Hu, Y. C.; Song, Q. L.; *Catal. Lett.* **2009**, *132*, 64.
13. Triantafillidis, C. S.; Vlessidis, A. G.; Nalbandian, L.; Evmiridis, N. P.; *Microporous Mesoporous Mater.* **2001**, *47,* 369.
14. Motz, J. L.; Heinichen, H.; Hölderich, W. F.; *J. Mol. Catal. A: Chem.* **1998**, *136*, 175.
15. Zhan, N. N.; Hu, Y.; Li, H.; Yu, D. H.; Han, Y. W.; Huang, H.; *Catal. Commun.* **2010**, *11*, 633.
16. Ramesh, K.; Hui, L. M.; Han, Y. F.; *Catal. Commun.* **2009**, *10*, 567.
17. Ogura, M.; Shinomiya, S. Y.; Tateno, J.; *Appl. Catal., A* **2001**, *219*, 33.
18. Suzuki, T.; Okuhara, T.; *Microporous Mesoporous Mater.* **2001**, *43,* 83.
19. Groen, J. C.; Pérez-Ramfrez, J.; Peffer, L. A. A.; *Chem. Lett.* **2002***, 31*, 94.
20. Groen, J. C.; Peffer, L. A. A.; Moulijn, J. A.; Pérez-Ramfrez, J.; *Microporous Mesoporous Mater.* **2004**, *69,* 29.
21. Cizmek, A.; Subotic, B.; Aiello, R.; Crea, F.; Nastro, A.; Tuoto, C.; *Microporous Mater.* **1995**, *4,* 159.
22. Jin, L. J.; Zhou, X. J.; Hu, H. Q.; Ma, B.; *Catal. Commun.* **2008**, *10*, 336.
23. Song, Y. Q.; Zhu, X. X.; Song, Y.; Wang, Q. X.; Xu, L. Y.; *Appl. Catal., A* **2006**, *302*, 69.
24. Bjørgen, M.; Joensen, F.; Holm, M. S.; Olsbye, U.; Lillerud, K. P.; Svelle, S.; *Appl. Catal., A* **2008**, *345*, 43.
25. Gayubo, A. G.; Alonso, A.; Valle, B.; Aguayo, A. T.; Bilbao, J.; *Appl. Catal., B* **2010**, *97*, 299.
26. Groen, J. C.; Peffer, L. A. A.; Moulijn, J. A.; Pérez-Ramfrez, J.; *Colloids Surf., A* **2004**, *241*, 53.
27. Jung, J. S.; Park, J. W.; Seo, G.; *Appl. Catal., A* **2005***, 288*, 149.
28. Li, Y. N.; Liu, S. G.; Zhang, Z. K.; Xie, S. J.; Zhu, X. X.; Xu, L. Y.; *Appl. Catal., A* **2008**, *338*, 100.
29. Groen, J. C.; Moulijn, J. A.; Pérez-Ramfrez, J.; *Microporous Mesoporous Mater.* **2005**, *87,* 153.
30. Song, Y. Q.; Feng, Y. L.; Liu, F.; Kang, C. L.; Zhou, X. L.; Xu, L. Y.; Yu, G. X.; *J. Mol. Catal. A: Chem.* **2009**, *310*, 130.
31. Groen, J. C.; Moulijn, J. A.; Pérez-Ramfrez, J.; *J. Mater. Chem.* **2006**, *16*, 2121.
32. Christensen, C. H.; Johannsen, K.; Toernqvist, E.; Schmidt, I.; Topsoe, H.; *Catal. Today* **2007**, *128*, 117.
33. Lu, M.; Sun, H. M.; Guo, Y.; Yang, W. M.; Zhu, Z. B.; *Acta Pet. Sin. (Petroleum Processing Section)* **2001**, *17,* 59.
34. Jiang, Y.; Liang, J.; Zhao, S. Q.; *Chin. J. Catal.* **1994**, *15*, 463.
35. Nguyen, T. A. M.; Mao, R. Le Van; *Appl. Catal.* **1990**, *58*, 119.
36. Varisli, D.; Dogu, T.; Dogu, G.; *Chem. Eng. Sci.* **2009***, 65, 153.*
37. Bedia, J.; Barrionuevo, R.; Rodríguez-Mirasol, J.; Cordero, T.; *Appl. Catal., B* **2011**, *103*, 302.
38. Wang, F.; Luo, M.; Xiao, W. D.; Cheng, X. W.; Long, Y. C.; *Appl. Catal.* **2011**, *393*, 161.
39. Zhou, L. W.; Wang, F.; Luo, M.; Xiao, W. D.; Cheng, X. W.; Long, Y. C.; *Petrochem. Technol.* **2008**, *37*, 333.

Submitted on: December 3, 2013
Published online: May 27, 2014